

1 *A manuscript re-submitted to* Environmental Microbiology (Microbiology of low water-
2 activity habitats)

3

4 **Retinal-binding proteins mirror prokaryotic** 5 **dynamics in multi-pond solar salterns**

6 María Gomariz^{1,2}, Manuel Martínez-García², Fernando Santos², Marco Constantino²,
7 Inmaculada Meseguer¹ and Josefa Antón^{2*}

8 ¹ Department of Materials, Optics and Electronics, University Miguel Hernández of Elche,
9 Alicante, Spain.

10 ² Department of Physiology, Genetics, and Microbiology, University of Alicante, 03080
11 Alicante, Spain

12 *Correspondence to: Josefa Antón, Department of Physiology, Genetics and Microbiology,
13 University of Alicante, 03080 Alicante, Spain.

14 Phone: +34965903870, E-mail: anton@ua.es

15

16

This article has been accepted for publication and undergone full peer review but has not been through the copyediting, typesetting, pagination and proofreading process, which may lead to differences between this version and the Version of Record. Please cite this article as doi: 10.1111/1462-2920.12709

1

This article is protected by copyright. All rights reserved.

17

18 **Summary**

19 Microbial opsin (i.e. retinal-binding protein) dynamics has been studied along a salinity
20 gradient in Santa Pola solar salterns (Alicante, Spain) by using culture-independent
21 approaches and statistical analyses. Five ponds of salinities ranging from 18% to above
22 40% were sampled nine times along a year. Forty three opsin-like sequences were retrieved
23 by denaturing gradient gel electrophoresis and clustered into 18 different phylogroups,
24 indicating that their diversity was higher than expected according to previous data.
25 Moreover, the statistical correlation between environmental factors controlling microbial
26 community structure and dynamics of environmental rhodopsin proteins indicated almost
27 identical temporal fluctuations between the opsin-related sequences and their
28 corresponding putative ‘producers’ in nature. Although most sequences were related to
29 others previously detected in hypersaline environments, some pond-specific opsins
30 putatively belonged to previously uncharacterized hosts. Furthermore, we propose that
31 subtle changes in the bacteriorhodopsin ‘retinal proton binding pocket’, which is key in the
32 photocycle function, could be the molecular basis behind a fine ‘photocycle-tuning’
33 mechanism to avoid inter/intra-species light-competition in hypersaline environments.

34

35

36 **Introduction**

37 Light-driven microbial rhodopsins are a widespread family of proteins whose function is to
38 transform visible light into a physiological response. Rhodopsins are formed by a seven-
39 helix transmembrane protein bound to a retinal chromophore, and are widely distributed in
40 microorganisms inhabiting photic waters. Microbial retinal-binding proteins* (RBPs) in
41 hypersaline systems mainly include outward-directed proton pumps, such as
42 bacteriorhodopsin (BR) and related proteins, the inward-directed chloride pump
43 halorhodopsin (HR), and sensory rhodopsins involved in light sensing for phototaxis
44 (Oren, 2002). In these RBPs, light excites the retinal chromophore and subsequently a
45 change of the native protein configuration occurs in a cyclic succession of intermediate
46 states leading the photocycle process. As a result, certain ions are released through the cell
47 membrane to accomplish several functions, including ATP synthesis, flagellar motion or
48 osmoregulation. Other prokaryotic rhodopsins, currently under characterization, have been
49 recently detected, such as the xenorhodopin, a sensory RBP found in *Anabaena* sp.
50 (Ugalde *et al.*, 2011), and the NaR, a new type of microbial rhodopsin found in marine
51 Flavobacteria, which acts as a light-driven sodium pump (Inoue *et al.*, 2013).

52

53

54 *Note: The names BR, XR and ActR refer to the protein bound to retinal. The proper names of unbound
55 proteins are bacterio-opsin, xantho-opsin and actino-opsin. Here, with the exception of BR purified from
56 salterns, we work with the retinal-binding proteins coding genes and their translated sequences, which
57 subsequently lack retinal. However, to avoid a tedious system of symbols, the following abbreviations will be

58 used throughout the text: BR for bacteriorhodopsin/bacterio-opsin, XR for xanthorhodopsin/xantho-opsin,
59 ActR for actinorhodopsin/actino-opsin and RBP for the retinal-binding proteins as a whole.
60 Microbial rhodopsins were first discovered in extremely halophilic *Archaea*, such as
61 *Halobacterium salinarum*, and later in other members of the family Halobacteriaceae, such
62 as *Haloquadratum walsbyi*, the ‘square’ archaeon that dominates many hypersaline
63 environments (Bolhuis *et al.*, 2006). One of the best characterized archaeal rhodopsins is
64 BR, whose functional features, together with the photoelectric, photochemical and
65 photochromic properties, make it a suitable model for applied technologies, such as optic
66 sensors and artificial retina (Birge *et al.*, 1999; Hampp *et al.*, 2000; Wagner *et al.*, 2013).
67 In the past decades, new types of light-driven proton pumping proteins, analogous to BR,
68 were also found in the bacterial domain: proteorhodopsin (PR), xanthorhodopsin (XR) and
69 actinorhodopsin (ActR). PRs were discovered in the surface waters of the oceans by means
70 of metagenomics (Béja, 2001; Rusch *et al.*, 2007; Fuhrman *et al.*, 2008). XR is produced
71 by *Salinibacter ruber* (Balashov *et al.*, 2005), an extremely halophilic bacterium broadly
72 distributed among different hypersaline environments (Antón *et al.*, 2000, 2002, 2008).
73 XR, besides the retinal chromophore, possesses the carotenoid salinixanthin acting as light-
74 harvesting antenna and providing energy from a wider spectral range (Balashov *et al.*,
75 2005). Although in past years several XR-coding genes have been found in
76 *Gammaproteobacteria*, *Flavobacteria* or *Betaproteobacteria* members (López-Pérez *et al.*,
77 2013; Riedel *et al.*, 2013; Oh *et al.*, 2011), there is no evidence of a light-harvesting
78 carotenoids in any of them yet. More recently, ActRs, associated with uncultured
79 *Actinobacteria* have been recovered from freshwaters, estuarine and lagoon sites (Sharma
80 *et al.*, 2007, 2008) and also from hypersaline waters (Ghai *et al.*, 2011).

81 Many rhodopsins from halophilic microorganisms (Otomo *et al.*, 1992; Kamekura *et al.*,
82 1998; Yatsunami *et al.*, 2000; Brown *et al.*, 2001; Balashov *et al.*, 2005; Luecke *et al.*,
83 2008) have been exhaustively characterized. However, only a few studies have been
84 focused on natural ecosystems. In particular, Oren (1983) and Javor (1983) analyzed the
85 BR production by the haloarchaeal populations inhabiting two hypersaline environments:
86 The Dead Sea and Guerrero Negro saltern ponds (Baja CA Sur, Mexico), respectively.
87 Later, Papke *et al.*, (2003) and Pašić *et al.*, (2005) studied the diversity of BR genes in
88 Mediterranean and Adriatic solar salterns, respectively. Recently, Dillon *et al.*, (2013)
89 studied the prokaryotic community structure and the BR genes recovered from three ponds
90 of increasing salinity in the Exportadora de Sal (ESSA) salterns (Baja CA, MX), finding
91 new bacterio-opsins, some of them “pond-specific”.

92 Here, we have analyzed RBP diversity in five hypersaline interconnected ponds of
93 increasing salinity from Santa Pola salterns (Spain), spanning a salt gradient from 18% to
94 more than 40%. These ponds were two medium concentrators (CMs: CM1 and CM2), a
95 brine concentrator (CCAB), and two crystallizers (CRs: CR30 and CR41). Previously, we
96 had studied the particular physicochemical and microbial diversity characteristics of these
97 same five ponds (Gomariz *et al.*, 2014) and found that the microbial community structure
98 was strongly correlated with ionic composition and meteorological factors (Gomariz *et al.*,
99 2014). The microbial community was dominated by the well-known halophilic prokaryotes
100 *Hqr. walsbyi* and *S. ruber*, together with members of the recently reported groups of
101 uncultured *Nanohaloarchaeota*, low GC *Actinobacteria* and a new group of ubiquitous,
102 previously unrecognized *Bacteroidetes* generalists. In addition, our data indicated that

103 although both crystallizers were fed with the same water, different “pond-specific”
104 phylotypes were detected together with significant variations in microbial community
105 structure and temporal dynamics. Overall, we observed that variation in archaeal and
106 bacterial diversity was much higher than expected for solar salterns, considered to date as
107 steady-state systems.

108 The main goal of the work presented here was to assess RBP temporal dynamics along a
109 year and correlate it with microbial dynamics and environmental parameters. Overall, we
110 found that RBP diversity followed the same trends as their putative microbial producers. In
111 addition, some of the BR-like sequences obtained displayed amino acid changes in
112 homologous positions of the predicted ‘retinal-binding pocket’ which could be involved in
113 photocycle-tuning mechanisms.

114

115 **Results and discussion**

116 *Diversity of archaeal bacteriorhodopsins and BR quantification in solar saltern ponds*

117 Around 30 sequences related to genes coding for bacteriorhodopsins were obtained from
118 the DGGE analysis (Figure S1; see experimental procedures for more details). These
119 sequences were clustered into 16 groups according to their phylogenetic relatedness based
120 on nucleotide similarities (Table S1). Each one of the resulting groups corresponded to a
121 single and robust branch (hereafter named as ‘phylogroup’) in the phylogenetic tree shown
122 in Figure 1. As shown in Table 1 and Figure 1, a large proportion (80%) of BR-like
123 sequences, recovered in nearly all the samples, were clearly related to *Hqr. walsbyi*
124 bacterio-opsin SbopI (phylogroups 9 to 15) and *Halorubrum* sp. archeo-opsin (groups 1

125 and 6) with amino acid similarities above 60% in the fragment analyzed. Sequences from
126 phylogroups 2 to 5 were, surprisingly, related to BR-genes from microorganisms which
127 had not been previously detected in these samples by 16S rRNA gene amplification
128 (Gomariz *et al.*, 2014), such as *Natrinema*, *Halosimplex*, *Halonotius* and *Halorhabdus*
129 representatives. These rhodopsins were only retrieved from specific ponds in a few
130 samples (see Table 1).

131 Around 7% of the RBP sequences obtained in this work (Table 1) had been previously
132 detected in Santa Pola salterns (Papke *et al.*, 2003). In the case of BR sequences, despite
133 the geographical distance, \approx 20% and 60% of the sequences were similar to those from
134 Lake Tyrrell in Australia (Podell *et al.*, 2013) and ESSA saltern ponds in Baja California,
135 Mexico (Dillon *et al.*, 2013).

136 In addition to the diversity study, an analysis of the BR protein production was
137 accomplished by SDS-PAGE (Figure S2), where a highly stained protein band of nearly
138 26 kDa (molecular weight determined for purified BRs) was detected in all the samples
139 analyzed. MALDI-TOF analysis showed a peptide sequence (9 amino acids) identical to a
140 fragment of the 'chain A' present in the BR (SbopI) from *Hqr. walsbyi*. Given that SbopI
141 is a predominant protein in the *Hqr. walsbyi* membrane (Fusetti and Poolman,
142 unpublished), and this haloarchaeon represents up to 60% of the microbial communities in
143 evaporation ponds from solar salterns (Antón *et al.*, 1999), it is very likely that the
144 observed 26 kDa band corresponds indeed to SbopI.

145 The concentration of bacteriorhodopsin in the analyzed samples, determined by
146 densitometry from SDS-PAGE images, ranged from 20 to 340 μ g/ml (Table S2). The

147 highest amounts of BR corresponded to the summer samples (June 1, June 2 and July)
148 from the crystallizer ponds CR30 and CR41. As discussed below, there was a strong
149 correlation between BR production, PAR, salinity and archaeal numbers, whose values
150 were very high in these summer samples. Previous works in the Dead Sea and Guerrero
151 Negro saltworks (Javor *et al.*, 1983; Oren *et al.*, 1983) attributed the high BR concentration
152 to the oligotrophic nature of these environments. The crystallizer pond waters studied here
153 contained considerable amounts of both organic and inorganic nutrients, as well as dense
154 prokaryotic communities (Gomariz *et al.*, 2014, and unpublished results). However,
155 according to Burns and colleagues (2007), magnesium ions, that can reach up to 2 M in
156 these environments (Gomariz *et al.*, 2014), could form complexes with dissolved nutrients,
157 decreasing their availability to microbes. In addition, oxygen solubility decreases in these
158 extremely hypersaline ponds. The combination of these factors could act in promoting the
159 production of BR to obtain an additional energy supply.

160 Finally, it is also known that members from the recently described phylum
161 Nanohaloarchaeota have been shown to present a photoheterotrophic lifestyle (Ghai *et al.*,
162 2011) since they present genes which would code for BR proteins. We did not detect
163 nanohaloarchaeal rhodopsin sequences since the PCR primers used here were designed
164 before the discovery of this phylum in 2012.

165 ***Diversity of bacterial rhodopsins***

166 After DGGE analysis, 13 sequenced bands were related to bacterial rhodopsins (Figures
167 S3-4): XR (9 bands) and ActR (4 bands) (Table 1). XRs were detected in all the samples
168 analyzed (Figure S3) and were all classified into one group according to their relatedness.

169 XR sequences showed amino acid similarities between 91% and 100% with *S. ruber* XR,
170 thus suggesting that they most likely correspond to *Salinibacter* producers. However, it is
171 possible that some of them could be related to different bacteria. In fact, it has been
172 recently discovered by means of single-cell genomics, that the ubiquitous hyperhalophilic
173 *Bacteroidetes* phylotype BC3, present in Santa Pola salterns, harbors a XR-coding gene
174 (Gomariz *et al.*, 2014; SAG AB577010). Other halophilic bacteria, such as the recently
175 described *Spiribacter* sp. (a moderately halophilic Gammaproteobacterium), also possesses
176 XR (López-Pérez *et al.*, 2013). However, *Spiribacter* representatives were not detected in
177 the ponds analyzed here and its XR presents a similarity below 50% when compared with
178 the *S. ruber* XR.

179 The ActR sequences obtained here were related (77-81% similarities) to the
180 actinorhodopsin of *Candidatus 'Aquiluna rubra'*, isolated from arctic fjord seawaters
181 (Kang *et al.*, 2012). ActR sequences were detected from spring to early summer only in
182 low-medium salinity ponds CM1 and CM2 (212.5 to 350.13 g/L total salts) (Figure S4).
183 However, the detection of *Actinobacteria*-related phlotypes was not always coupled with
184 the presence of ActR sequences. One possible explanation for this paradox could rely on
185 the fact that ActR sequences are also known to be produced by *Gammaproteobacteria*, as
186 it occurs in other aquatic systems (Martinez-Garcia *et al.*, 2012), maybe due to lateral gene
187 transfer events, as dicussed below. Members of *Gammaproteobacteria* were detected in
188 CM ponds (Gomariz *et al.*, 2014).

189 ***Comparison between RBP and prokaryotic and environmental dynamics***

190 One of the main findings in this study was that both RBP and prokaryotic diversity
191 dynamics were nearly parallel in the five ponds analyzed (Figure 2). RBP and prokaryotic
192 diversities, determined by Shannon indices (H, Table S2), showed temporal fluctuations in
193 each pond. Low and medium salinity ponds (CMs and CCAB) showed higher BR and
194 archaeal diversity fluctuations than the crystallizers, which were more stable (Figure 2A).
195 In addition, the highest Shannon index H values for BR and *Archaea* were found in the
196 brine concentrator CCAB in June2 samples (H~2.2 for BR and H~2.4 for *Archaea*,
197 respectively). Equivalent H indices for BRs were also determined in another medium-high
198 salinity pond (Pond 9) from ESSA salterns (Dillon *et al.*, 2013) while lower indices
199 (H~1.4) had been previously observed in a ‘single-sample’ study carried out in Santa Pola
200 and Portoroz salterns (Papke *et al.*, 2003, Pašić *et al.*, 2005).

201 Data from both the prokaryotic community of Santa Pola salterns (Gomariz *et al.*, 2014)
202 and rhodopsin diversity were arranged according to their environmental optima as a result
203 of the CCA analysis (Figure 3 and Table S3). The term "optima" does not refer to growth
204 parameters but to the biplot site where a particular phylotype presents the highest
205 possibility to be found. In the CCA biplots: (i) those sequences located in the center of the
206 diagram correspond to sequences retrieved from nearly all the samples; (ii) the distance
207 between two sequences represents the probability of recovering them from the same
208 sample given that they share their environmental optima; and (iii) the relative position of
209 RBP and 16S rRNA sequences allows the suggestion of the relationship between
210 rhodopsins and their putative producers. For instance, in the CCA space, a given
211 *Haloquadratum* phylotype would be the most likely “producer” of its closest BR sequence.

212 Accordingly, different *Haloquadratum* and *Halorubrum*-related phlotypes appeared near
213 their respective BRs, along the salinity gradient (Figure 3). These results were in
214 agreement with previous diversity studies where *Sbop* gene clone libraries retrieved the
215 expected sequences according to the analysis of the 16S rRNA genes (Papke *et al.*, 2003,
216 Pašić *et al.*, 2005). However, there were also some intriguing findings since some of our
217 RBP sequences were related to microorganisms that had not been detected in the same
218 samples by the 16S rRNA approach, as discussed above and as was also reported by Dillon
219 *et al.*, (2013). Some of these “orphan” RBPs were pond-specific and month-specific (Table
220 1). Together with database limitations, this finding could be due to lateral transfer of RBP
221 coding genes. Indeed, it is well known that microbial rhodopsins present a patchy
222 distribution in prokaryotes (Frigaard *et al.*, 2006), and in particular, in haloarchaeal
223 lineages, due to lateral gene transfer processes (Sharma *et al.*, 2007). This mechanism
224 allows the organisms receiving RBP-coding genes to exploit more efficiently the energy
225 sources available in the environment.

226 Contrary to BR, XR diversity was quite stable over the year in all the samples although the
227 diversity of *Salinibacter*-related phlotypes was increasing along the salinity gradient
228 (Figure 2B). Indeed, most of the obtained XR sequences were located in the center of the
229 CCA diagram (Figure 3), showing their widespread distribution in the analyzed ponds.
230 This observation could be indicating that, as discussed above, other bacterial members,
231 apart from *Salinibacter* representatives, could contain XR-coding genes. Sequences related
232 to ActR were placed, as expected, next to actinobacterial phlotypes in the low salinity
233 optima conditions from the CCA biplot.

234 Regarding the biological-environmental data relationships, redundancy detrended analysis
235 (RDA) showed that the ionic composition (especially ammonium concentration), together
236 with PAR and the light hours per day, were the most significant environmental parameters
237 affecting the BR production in the ponds analyzed (Figure 4 and Table S4). Besides
238 salinity, meteorological factors were highly correlated with RBP diversity, prokaryotic
239 community abundance and prokaryotic diversity as well. In particular, BR and archaeal
240 diversities, as well as archaeal numbers, were strongly correlated with light, temperature
241 and solar radiation (Gomariz *et al.*, 2014). However, bacterial rhodopsin diversities were
242 negatively correlated with bacterial diversity and showed a highly positive correlation with
243 calcium concentration and bacterial counts.

244 ***“Photocycle-tuning” of BR-like proteins***

245 BR alignments revealed that some of the amino acids in the obtained sequences changed
246 with respect to the closest rhodopsin relatives available in databases. Over the years, it has
247 been demonstrated that changes affecting certain amino acids could lead to changes in the
248 rhodopsin photocycle, such as displacement of the maximum absorption peak,
249 modification of the average life of the intermediates in the photocycle or a proton-pumping
250 direction inversion (Brown *et al.*, 2001; Luecke *et al.*, 2001; Sanz *et al.*, 2001; Chaumont
251 *et al.*, 2008, Sudo *et al.*, 2011).

252 In our study, although some amino acids involved in the ‘retinal-binding pocket’ (Trp137,
253 Trp182, Trp189, Thr89 and Asp115) were quite conserved, others (such as Glu194-
254 Gly200, in helix loop F-G, and Glu204-Val210, in helix G) presented modifications which
255 could play an important role in the photocycle. In particular, Glu194, Gly200 and Glu204

256 are known to be important residues in transduction signaling, color tuning or in the
257 regulation of certain functions such as energy production and motility (Shimono *et al.*,
258 2003; Sanz *et al.*, 2011; Sudo *et al.*, 2006; Sudo *et al.*, 2011). Other amino acids, such as
259 Arg82 and Trp86 (in helix C), also play an important role in proton channel release;
260 however, we did not analyze this region of the protein since the amplified BR fragment
261 ranged from amino acid 90 to position 222. Taking into account the amino acid
262 similarities, our BR sequences were clustered in different groups (0-XIII), corresponding
263 to different putative types with respect to their response to light. Therefore, we will refer to
264 these ‘functional groups’ as ‘photocycle-tuning’ varieties based on their changed amino
265 acids (Table 2).

266 The relationship between BR phylogroups and functional varieties showed some
267 interesting features. For instance, sequences related to SboptI, within phylogroup 11,
268 presented different functional varieties (functional groups 0 and VII in Figure 1). In the
269 environment, this fact could probably portray a scenario where different *Haloquadratum*
270 coexisting lineages would be differentially specialized in the use of light in order to avoid
271 direct intraspecific competition, as discussed in Legault *et al.* (2006) and Cuadros-Orellana
272 *et al.* (2007). Additionally, specific BR sequences related to different species (e.g.
273 *Halorubrum* spp. and *Haloquadratum* spp.) and thus clustered in different phylogroups
274 (phylogroups 6 and 7, respectively), belonged to the same functional group XIII. Indeed,
275 this variety (group XIII) was the most widely distributed among the saltern ponds analyzed
276 (Figure 5); while the remaining varieties presented a particular distribution along the
277 different environmental gradients (Figures 2 and 5). In addition, the CCA analysis (Figure

278 3) revealed that meteorological factors were correlated with the occurrence of the different
279 varieties. For instance, two *Halorubrum* BR-related sequences (25br5 and 23br3), included
280 in the same phylogroup (6) but in different functional varieties (XI and VI), were detected
281 in different and opposite temperature optima conditions (Figure 3). Therefore, even though
282 no significant temporal variations of phylogroup diversity was observed (Figure S5), we
283 detected temporal fluctuations of the functional varieties (Figure 4). This points to a fine
284 tuning of light exploitation which is most likely driven by environmental conditions.

285 **Conclusion**

286 The present study shows coherent spatial and temporal parallelisms between retinal-
287 binding proteins and prokaryotic communities in solar salterns. A high number of different
288 opsin-coding gene sequences has been successfully collected, mainly because this work
289 has been carried out over a wide period of time. In fact, as Dillon and colleagues (2013)
290 suggested “a global undersampling could be the main reason of a currently limited ‘bop’
291 environmental data set”. Our results point to the existence of a spatial and temporal
292 arrangement of different ‘functional varieties’ of BRs that could be part of a strategy to
293 avoid light-competition in saturated brines. Future studies could thus focus on elucidating
294 the implications of this “photocycle-tuning” in light-adaptation strategies of both bacterial
295 and archaeal rhodopsin producers in hypersaline environments.

296 **Experimental procedures**

297 *Collection and characterization of samples*

298 Samples from five interconnected ponds of increasing salinity (CM1, CM2, CCAB , CR30
299 and CR41) from Santa Pola saltworks were taken during 2006, on the following dates: 23

300 January (JN), 7 March (MR), 26 April (AP), 6 June (J1), 27 June (J2), 25 July (JL), 5
301 September (SP), 2 October (OC) and 28 November (NV). Changes in prokaryotic
302 communities in these samples and their relationship with 16 different environmental
303 parameters have been described previously (Gomariz *et al.*, 2014).

304 ***Bacteriorhodopsin quantification***

305 Environmental water samples (500 ml) were centrifuged at 16,000 rpm (rotor JLA-16,
306 centrifuge Beckman Coulter Avanti J-25) 15 min, at 4°C. Then, pellet cells were washed
307 and concentrated in basal salt solution, 500 µl SW25% (Rodríguez-Valera *et al.*, 1983).
308 Subsequently, cells were centrifuged at 13,000 rpm (Biofuge, HERAUS) and lysed in 500
309 µl mQ water. Then, cells lysates were sonicated (Bandelin electronic, Sonoplus GM2200)
310 in three cycles of 5 s in ice to avoid heating of the membranes. Finally, membrane
311 suspensions were lyophilized (Telstar, Cryodos 5) and kept at -20°C until their
312 electrophoretic analysis.

313 Total membrane proteins (50 µg) from environmental samples were separated by sodium
314 dodecyl sulphate polyacrylamide gel electrophoresis (SDS-PAGE) following the protocol
315 described in Laemmli *et al.* (1970). For each sample, two different amounts of protein (25
316 µg and 50 µg, dry weight) were analyzed. For one of the samples, a protein band with a
317 molecular weight similar to that of bacteriorhodopsin (26 kDa) was cut with a sterile
318 blade and analyzed by Matrix Assisted Laser Desorption Ionization Time-of-Flight
319 (MALDI-tof), which unambiguously indicated the presence of a BR-like peptide. Thus,
320 based on these results, we assumed that all the bands with the expected molecular weight

321 corresponded to BR. BR concentration was estimated by densitometry of these bands in
322 SDS-PAGE images by means of the LabWorks 4.0 software (UVP).

323 ***PCR-DGGE analysis of rhodopsin genes***

324 DNA purified (100 ng) extracted from environmental samples as described in Gomariz *et*
325 *al.*, 2014, was used to amplify RBP coding genes using specific primers designed in this
326 study (Table S5). Each PCR reaction contained MgCl₂ 1.5 mM, Tris-HCl 10 mM pH 9.0,
327 KCl 50 mM, 200 μM of each dNTP (deoxynucleotide triphosphate), 0.2 M of each primer,
328 1 U Taq DNA polymerase I and DNA template (100 ng) in a final volume of 50 μl. Each
329 PCR reaction was performed in a PTC-100 (Peltier-Effect Cycling) using PCR programs
330 specific for each amplified gene (see Table S6 for more details). After amplification, the
331 presence of heteroduplex and chimeric molecules was minimized by a ‘reconditioning
332 PCR’ step (Thompson *et al.*, 2002). Finally, the ‘reconditioned’ PCR products were
333 purified with the Gel Band Purification Kit (GE Healthcare) and quantified by using a
334 NanoDrop ND-1000 spectrophotometer (Thermo Fisher Scientific).

335 DGGE was performed by using the D-Code System (Bio-Rad). PCR products were loaded
336 onto 6% (w/v) polyacrylamide gels with 45% to 65% urea-formamide denaturing gradient
337 in 1X TAE buffer and subjected to 16-18 h of electrophoresis at 60 °C and 70 V. After
338 electrophoresis, the gels were stained with SYBR Green (1:10,000) (Fluka) for 15 min,
339 washed in TAE 1X for 30 minutes and visualized using a computer image analyzer
340 Typhoon 9410 (Amersham Biosciences). Nearly all different bands were cut, and re-
341 amplified with the same primer pairs. Then a DGGE was run to check that each band
342 corresponded to a single PCR product. Bands were then, checked for presence of single

343 band by DGGE and then sequenced at the Technical Services Unit of the University of
344 Alicante using a GeneAmp PCR System 2400 and an ABI PRISM 310 Genetic Analyzer
345 (Applied Biosystems). The obtained rhodopsin sequences were compared with the
346 GenBank protein database using the BLASTx software at the National Center of
347 Biotechnology Information website (<http://www.ncbi.nlm.nih.gov/>) (Altschul *et al.*, 1997).
348 These sequences have been deposited in the GenBank database with Accession Numbers
349 KM226176- KM226204, KM226164- KM226171, KM226172- KM226175 for BR, XR
350 and ActR sequences, respectively. Finally, RBP sequences were classified in different
351 groups according to their phylogenetic signals and a maximum likelihood (ML) tree was
352 constructed (100 bootstrap replicates) using Geneious 6.0 software Biomatters, Ltd
353 (www.geneious.com) in order to evaluate the evolutionary relationships among them.
354 Additionally, bacteriorhodopsin nucleotide sequences were translated using Expasy
355 translate tool (www.expasy.org/translate) and aligned with database bop sequences by
356 means of Clustal Omega software program (<http://www.ebi.ac.uk/Tools/msa/clustalo/>) in
357 order to analyze changes in retinal-binding pocket amino acids.

358 ***Multivariate statistical analysis***

359 In order to correlate the biological data (bacterial and archaeal abundances, amount of BR,
360 prokaryotic and rhodopsin diversities) with environmental parameters (temperature, pH,
361 salinity and sodium, potassium, calcium, magnesium, ammonium, sulfate, chloride,
362 carbonate and phosphate concentration) from Gomariz *et al.*, (2014), redundancy detrended
363 analysis (RDA) and canonical correspondence (CCA) multivariate analyses were carried
364 out using the CANOCO 4.5 software package program (ter Braak and Smilauer, 2002).

365 **Acknowledgements**

366 This work was supported by project CGL2012-39627-C03-01 of the Spanish Ministry of
367 Economy and Competitiveness, which was also co-funded with FEDER support from the
368 European Union. We thank the staff of the Bras del Port salterns for their help throughout
369 the sampling campaign. The authors declare no conflict of interest.

370 **References**

371 Altschul, S. F., Madden, T. L., Schäffer, A. A., Zhang, J., Zhang, Z., Miller, W., and
372 Lipman, D. J. (1997) Gapped BLAST and PSI-BLAST: a new generation of protein
373 database search programs. *Nucleic Acids Res* **25**:3389-402.

374 Antón, J., Llobet-Brossa, E., Rodríguez-Valera, F., and Amann, R. (1999) Fluorescence in
375 situ hybridization analysis of the prokaryotic community inhabiting crystallizer
376 ponds. *Environ Microbiol* **1**: 517-23.

377 Antón, J., Rosselló-Mora, R., Rodríguez-Valera, F., and Amann, R. (2000) Extremely
378 halophilic bacteria in crystallizer ponds from solar salterns. *Appl Environ*
379 *Microbiol* **66**: 3052-7.

380 Antón, J., Oren, A., Benlloch, S., Rodríguez-Valera, F., Amann, R., and Rosselló-Mora, R.
381 (2002) *Salinibacter ruber* gen. nov., sp. nov., a novel, extremely halophilic member of
382 the *Bacteria* from saltern crystallizer ponds. *Int J Syst Evol Microbiol* **52**: 485-91.

383 Antón, J., Peña, A., Santos, F., Martínez-García, M., Schmitt-Kopplin, P., and Rosselló-
384 Mora, R. (2008). Distribution, abundance and diversity of the extremely halophilic
385 bacterium *Salinibacter ruber*. *Saline Systems* **28**:4-15.

386 Balashov, S. P., Imasheva, E. S., Boichenko, V. A., Anton, J., Wang, J. M., and Lanyi, J.
387 K. (2005) Xanthorhodopsin: a proton pump with a light-harvesting carotenoid
388 antenna. *Science* **309**: 2061-2064.

389 Béja, O., Spudich, E. N., Spudich, J. L., Leclerc, M., and DeLong, E. F. (2001)
390 Proteorhodopsin phototrophy in the ocean. *Nature* **411**: 786-789.

391 Birge, R. R., Gillespie, N. B., Izaguirre, E. W., Kusnetzow, A., Lawrence, A. F., Singh, D.
392 *et al.* (1999) Biomolecular electronics: protein-based associative processors and volumetric
393 memories. *J Phys Chem B* **103**: 10746-10766.

394 Burns, D.G, Janssen, P.H, Itoh. T., Kamekura. M., Li, Z., Jensen G *et al.* (2007)
395 *Haloquadratum walsbyi* gen. nov., sp. nov., the square haloarchaeon of Walsby, isolated
396 from saltern crystallizers in Australia and Spain. *Int J Syst Evol Microbiol* **57**:387-92.

397 Bolhuis, H., Palm, P., Wende, A., Falb, M., Rampp, M., Rodriguez-Valera, F. *et al.* (2006)
398 The genome of the square archaeon *Haloquadratum walsbyi*: life at the limits of water
399 activity. *BMC Genomics* **7**:169.

400 Brown, L. (2001) Proton transport mechanism of bacteriorhodopsin as revealed by site-
401 specific mutagenesis and protein sequence variability. *Biochemistry (Mosc)* **66**: 1249-
402 1255.

403 Chaumont, A., Baer, M., Mathias, G., and Marx, D. (2008) Potential Proton-Release
404 Channels in Bacteriorhodopsin. *ChemPhysChem* **9**: 2751-2758.

405 Cuadros-Orellana, S., Martin-Cuadrado, A., Legault, B., D'Auria, G., Zhaxybayeva, O.,
406 Papke, R. T., and Rodriguez-Valera, F. (2007) Genomic plasticity in prokaryotes: the case
407 of the square haloarchaeon. *ISME J* **1**: 235-245.

408 Dillon, J. G., Carlin, M., Gutierrez, A., Nguyen, V., and McLain, N. (2013) Patterns of
409 microbial diversity along a salinity gradient in the Guerrero Negro solar saltern, Baja CA
410 Sur, Mexico. *FMICB* **4**: 399.1-13.

411 Frigaard, N., Martinez, A., Mincer, T. J., & DeLong, E. F. (2006) Proteorhodopsin lateral
412 gene transfer between marine planktonic Bacteria and Archaea. *Nature* **439**: 847-850.

413 Fuhrman, J. A., Steele, J. A., Hewson, I., Schwalbach, M. S., Brown, M. V., Green, J. L.,
414 and Brown, J. H. (2008) A latitudinal diversity gradient in planktonic marine
415 bacteria. *Proc Natl Acad Sci U S A* **105**: 7774-7778.

416 Ghai, R., Pašić, L., Fernández, A.B., Martin-Cuadrado, A.B., Mizuno, C.M., McMahon
417 KD *et al.* (2011) New abundant microbial groups in aquatic hypersaline environments. *Sci*
418 *Rep Nature* **1**:135.

419 Gomariz, M., Martinez-Garcia, M., Santos, F., Rodriguez, F., Capella-Gutierrez, S.,
420 Gabaldon, T. *et al.* (2014) From community approaches to single-cell genomics: the
421 discovery of ubiquitous hyperhalophilic *Bacteroidetes* generalists. *ISME J.* doi:
422 10.1038/ismej.2014.95 in press.

423 Hampp, N. (2000) Bacteriorhodopsin as a photochromic retinal protein for optical
424 memories. *Chem Rev* **100**: 1755-1776.

425 Inoue, K., Ono, H., Abe-Yoshizumi, R., Yoshizawa, S., Ito, H., Kogure, K., and Kandori,
426 H. (2013) A light-driven sodium ion pump in marine bacteria. *Nat Commun* **4**: 1678.

427 Hammer, Ø., Harper, DAT., and Ryan PD. (2001). PAST: paleontological statistics
428 software package for education and data analysis. *Palaeontol Electron* **4**: 1.

429 Javor, B.J. (1983) Planktonic standing crop and nutrients in a saltern ecosystem. *Limnol.*
430 *Oceanogr.* **12**, 1-7.

431 Kamekura, M., Seno, Y., and Tomioka, H. (1998) Detection and expression of a gene
432 encoding a new bacteriorhodopsin from an extreme halophile strain HT (JCM 9743) which
433 does not possess bacteriorhodopsin activity. *Extremophiles* **2**: 33-40.

434 Kang, I., Lee, K., Yang, S. J., Choi, A., Kang, D., Lee, Y. K., and Cho, J. C. (2012)
435 Genome sequence of "Candidatus Aquiluna" sp. strain IMCC13023, a marine member of
436 the Actinobacteria isolated from an arctic fjord. *J Bacteriol* **194**: 3550-3551.

437 Laemmli, U. K. (1970) Cleavage of structural proteins during the assembly of the head of
438 bacteriophage T4. *Nature* **227**: 680-685.

439 Legault, B. A., Lopez-Lopez, A., Alba-Casado, J. C., Doolittle, W. F., Bolhuis, H.,
440 Rodriguez-Valera, F., and Papke, R. T. (2006) Environmental genomics of
441 "Haloquadratum walsbyi" in a saltern crystallizer indicates a large pool of accessory genes
442 in an otherwise coherent species. *BMC Genomics* **7**: 171.

443 López-Pérez, M., Ghai, R., Leon, M. J., Rodríguez-Olmos, Á., Copa-Patiño, J. L., Soliveri,
444 J. *et al.* (2013) Genomes of "Spiribacter", a streamlined, successful halophilic
445 bacterium. *BMC Genomics* **14**: 787.

446 Luecke, H., Schobert, B., Lanyi, J. K., Spudich, E. N., and Spudich, J. L. (2001) Crystal
447 structure of sensory rhodopsin II at 2.4 angstroms: insights into color tuning and transducer
448 interaction. *Science* **293**: 1499-1503.

449 Luecke, H., Schobert, B., Stagno, J., Imasheva, E. S., Wang, J. M., Balashov, S. P., and
450 Lanyi, J. K. (2008) Crystallographic structure of xanthorhodopsin, the light-driven proton
451 pump with a dual chromophore. *Proc Natl Acad Sci U S A* **105**: 16561-16565.

452 Martinez-Garcia, M., Swan, B. K., Poulton, N. J., Gomez, M. L., Masland, D., Sieracki, M.
453 E., and Stepanauskas, R. (2012) High-throughput single-cell sequencing identifies
454 photoheterotrophs and chemoautotrophs in freshwater bacterioplankton. *ISME J* **6**: 113-23.

455 Oh, H. M., Lee, K., Jang, Y., Kang, I., Kim, H. J., Kang, T. W. *et al.* (2011) Genome
456 sequence of strain IMCC9480, a xanthorhodopsin-bearing betaproteobacterium isolated
457 from the Arctic Ocean. *J Bacteriol* **193**: 3421-11.

458 Oren, A. (1983) Bacteriorhodopsin-mediated CO₂ photoassimilation in the Dead
459 Sea. *Limnol Oceanogr* **28**: 33-41.

460 Oren, A. (2002) Pigments of halophilic microorganisms. In *Halophilic Microorganisms*
461 *and their Environments*. Dordrecht, Netherlands: Springer. pp 173-205.

462 Otomo, J., Urabe, Y., Tomioka, H., and Sasabe, H. (1992) The primary structures of
463 helices A to G of three new bacteriorhodopsin-like retinal proteins. *J Gen*
464 *Microbiol* **138**: 2389-2396.

465 Papke, R. T., Douady, C. J., Doolittle, W. F., and Rodríguez-Valera, F. (2003) Diversity of
466 bacteriorhodopsins in different hypersaline waters from a single Spanish saltern. *Environ*
467 *Microbiol* **5**: 1039-1045.

468 Pašić, L., Bartual, S. G., Ulrih, N. P., Grabnar, M., and Velikonja, B. H. (2005) Diversity
469 of halophilic archaea in the crystallizers of an Adriatic solar saltern. *FEMS Microbiol*
470 *Ecol* **54**: 491-498.

471 Podell, S., Ugalde, J. A., Narasingarao, P., Banfield, J. F., Heidelberg, K. B., and Allen, E.
472 E. (2013) Assembly-driven community genomics of a hypersaline microbial
473 ecosystem. *PLoS One* **8**: 1-12.

474 Riedel, T., Gómez-Consarnau, L., Tomasch, J., Martin, M., Jarek, M., González, J. M. *et*
475 *al.* (2013) Genomics and physiology of a marine *Flavobacterium* encoding a
476 proteorhodopsin and a xanthorhodopsin-like protein. *PloS One* **8**: e57487.

477 Rodríguez-Valera, F., Juez, G., and Kushner, D. (1983). *Halobacterium mediterranei* spec,
478 nov., a New Carbohydrate-Utilizing Extreme Halophile. *Syst Appl Microbiol* **4**: 369-381.

479 Rusch, D. B., Halpern, A. L., Sutton, G., Heidelberg, K. B., Williamson, S., Yooseph, S. *et*
480 *al.* (2007) The Sorcerer II global ocean sampling expedition: northwest Atlantic through
481 eastern tropical Pacific. *PLoS Biol* **5**: 0398-0431.

482 Sanz, C., Marquez, M., Peralvarez, A., Elouatik, S., Sepulcre, F., Querol, E. *et al.* (2001)
483 Contribution of extracellular Glu residues to the structure and function of
484 bacteriorhodopsin. Presence of specific cation-binding sites. *J Biol Chem* **276**: 40788-
485 40794.

486 Sharma, A. K., Walsh, D. A., Baptiste, E., Rodríguez-Valera, F., Doolittle, W. F., and
487 Papke, R. T. (2007) Evolution of rhodopsin ion pumps in haloarchaea. *BMC Evol*
488 *Biol* **7**: 79.

489 Sharma, A. K., Zhaxybayeva, O., Papke, R. T., and Doolittle, W. F. (2008)
490 Actinorhodopsins: proteorhodopsin-like gene sequences found predominantly in
491 non-marine environments. *Environ Microbiol* **10**: 1039-1056.

492 Shimono, K., Hayashi, T., Ikeura, Y., Sudo, Y., Iwamoto, M., and Kamo, N. (2003)
493 Importance of the broad regional interaction for spectral tuning in *Natronobacterium*
494 *pharaonis* phoborhodopsin (sensory rhodopsin II). *J Biol Chem* **278**: 23882-23889.

495 Sudo, Y., Furutani, Y., Kandori, H., and Spudich, J. L. (2006) Functional importance of the
496 interhelical hydrogen bond between Thr204 and Tyr174 of sensory rhodopsin II and its
497 alteration during the signaling process. *J Biol Chem* **281**: 34239-34245.

498 Sudo, Y., Ihara, K., Kobayashi, S., Suzuki, D., Irieda, H., Kikukawa, T. *et al.* (2011) A
499 microbial rhodopsin with a unique retinal composition shows both sensory rhodopsin II
500 and bacteriorhodopsin-like properties. *J Biol Chem* **286**: 5967-5976.

501 ter Braak, C.J.F., and Smilauer, P. 2002. CANOCO Reference Manual and CanoDraw for
502 Windows User's Guide: Software for Canonical Community Ordination (version 4.5).
503 New York, USA: Microcomputer Power.

504 Thompson, J.R., Marcelino, L.A., Polz, M.F. (2002) Heteroduplexes in mixed-template
505 amplifications: formation, consequence and elimination by 'reconditioning PCR'. *Nucleic*
506 *Acids Res.* **30**: 2083-2088.

507 Ugalde, J. A., Podell, S., Narasingarao, P., and Allen, E. E. (2011) Xenorhodopsins, an
508 enigmatic new class of microbial rhodopsins horizontally transferred between archaea and
509 bacteria. *Biol Direct* **6**: 1-8.

510 Yatsunami, R., Kawakami, T., Ohtani, H., and Nakamura, S. (2000) A novel
511 bacteriorhodopsin-like protein from *Haloarcula japonica* strain TR-1: gene cloning,
512 sequencing, and transcript analysis. *Extremophiles* **4**: 109-114.

513 Wagner, N. L., Greco, J. A., Ranaghan, M. J., and Birge, R. R. (2013) Directed evolution
514 of bacteriorhodopsin for applications in bioelectronics. *J R Soc Interface* **10**: 1-33.

515 **Figure legends**

516 Figure 1: Phylogenetic tree of bop sequences retrieved from five hypersaline saltern ponds.
517 Maximum likelihood (ML) tree was constructed with 100 bootstrap using Geneious 6.0
518 software. Each tree branch corresponds with 16 phylogroups while “photocycle-tuning”
519 are colored according to their proton pumping pocket amino acids changed (Table 2). Non-
520 colored sequences are shorter than the rest and PBP amino acids are not available to
521 evaluate possible changes.

522 Figure 2: Temporal variation of retinal-binding protein (dashed lines) with prokaryotic
523 community diversity in each pond from January to November in 2006. In panel A:
524 *Archaea* (black) and BR-like protein (white) diversity (circles); HQR-related phlotypes
525 (black) and SbpI-like protein (white) diversity (squares). In panel B: *Bacteroidetes*
526 (black) and *Proteobacteria* (gray) diversity (squares); *S. ruber* (black), XR-like,
527 xanthorhodopsin (white) diversity (circles). Finally, Actinobacteria (black) and ActR
528 (gray) diversity (asterisks). A Shannon index 0 value correspond to only one registered
529 OTU sequence, while empty samples are obviously non-sequence detection.

530 Figure 3: Canonical correspondence analysis (CCA) ordination biplot of phlotypes
531 (symbols) and environmental parameters (arrows) from Gomariz *et al.*, 2014. Retinal-
532 Binding Proteins (BR, XR and ActR; described in Table 1) are represented as colored
533 cross-hatched symbols with related phlotypes (archaeal in section A and bacterial in
534 section B).

535 Figure 4: Redundancy detrended analysis (RDA) canonical ordination biplot of
536 environmental and biological parameters. DAPI, *Archaea* and *Bacteria* abundances are
537 represented by the logarithm of the number of cells per milliliter and the prokaryotic
538 community (all of them taken from Gomariz *et al.*, 2014) and retinal-binding proteins (BR
539 and XR) diversity by Shannon diversity indices (H). RDA yielded two synthetic canonical
540 axes (RDA1 and RDA2) that explained 69.2% of data variance.

541 Figure 5. Spatio-temporal distribution of “Photocycle-tuning” varieties (detailed in Table
542 2) in each of the analyzed ponds.

Table 1: Retinal-binding coding protein sequences retrieved in this study. Closest cultured and uncultured relative similarities are indicated as well the pond and month where/when the sequences were detected in (Pond and month detected). Ponds: Medium concentrators, CMs (CM1 and CM2), brine concentrator, CCAB and crystallizers, CRs (CR30 and CR41).

BACTERIORHODOPSIN-LIKE PROTEIN							
Phylogroup	Photocycle-tuning protein	Sequences	Closest cultured relative (Genbank Access Number) Closest uncultured relative (Genbank Access Number)	Authors	Similarity (%)	Detected in	
						Pond	Month
1	III	18BR1	bacteriorhodopsin, partial [uncultured bacterium] (ADJ38522.1)	Dillon et al., 2013	89%	CM1 CM2	J1-J2 AB, J2-OC
			bacteriorhodopsin [<i>Halorubrum kocurii</i>] (WP_008848850.1)	Podell et al., 2013	69%		
2	VIII	19BR5	bacteriorhodopsin, partial [uncultured Halobacteriales archaeon] (AAZ76796.1)	Dillon et al., 2013	82%	CCAB	All months (except SP and NV)
			bacteriorhodopsin, partial [<i>Halorhabdus</i> sp. A001] (AGV98942.1)	Yang, J et al., unpublished	54%		
3	VI	19BR8	bacteriorhodopsin, partial [uncultured bacterium] (ADJ38539.1)	Dillon et al., 2013	55%	CCAB	J2-OC
			bacteriorhodopsin, partial [<i>Halosimplex carlsbadense</i>] (ABT17454.1)	Sharma et al., 2007	57%		
4	II	18BR3	bacteriorhodopsin, partial [uncultured haloarchaeon] (AHF27668.1)	Dillon et al., 2013	90%	CMs	J1-J2 and NV
			bacteriorhodopsin, partial [<i>Natrinema</i> sp. enrichment culture clone ABDH2] (ACO36736.1)	Tohty et al., 2009	67%		
5	XII	25BR4	bacteriorhodopsin [uncultured archaeon A07HN63] (WP_023502072.1)	Podell et al., 2013	91%	CR41	EN
			bacteriorhodopsin [<i>Halonotius</i> sp. J07HN4] (WP_021041057.1)	Burs et al., 2009	98%		
6	XIII	18BR6	bacteriorhodopsin, partial [uncultured haloarchaeon] (AGZ13717.1)	Dillon et al., 2013	73-96%	CM1	AB
	0	23BR3,4				CR30	JL-SP and NV
	XI	25BR5				bacteriorhodopsin [<i>Halorubrum californiense</i>] (WP_008440455.1)	Presente et al., 2008
7	XIII	23BR2	bacteriorhodopsin, partial [uncultured haloarchaeon] (AGZ13712.1)	Dillon et al., 2013	94-100%	CRs	Every months
		18BR5, 23BR9, 25BR2	bacteriorhodopsin precursor (Squarebop I) [<i>Haloquadratum walsbyi</i> DSM 16790](YP_656801.1)	Pfeiffer et al., 2008	58-62%	CM2 and CRs	Every months
8		19BR9	bacteriorhodopsin, partial [halophilic archaeon F7] (ABY53427.1)	Dillon et al., 2013	55%	CCAB	J2-NV
			bacteriorhodopsin, partial [<i>Natrinema altunense</i>] (AAS87571.1)	Xu et al., unpublished	55%		
9		25BR3	bacteriorhodopsin, partial [uncultured Halobacteriales archaeon] (AAR12473.1)	Papke et al., 2003	64%	CR41	Every months
			bacteriorhodopsin precursor (Squarebop I) [<i>Haloquadratum walsbyi</i> DSM 16790](YP_656801.1)	Pfeiffer et al., 2008	60%		

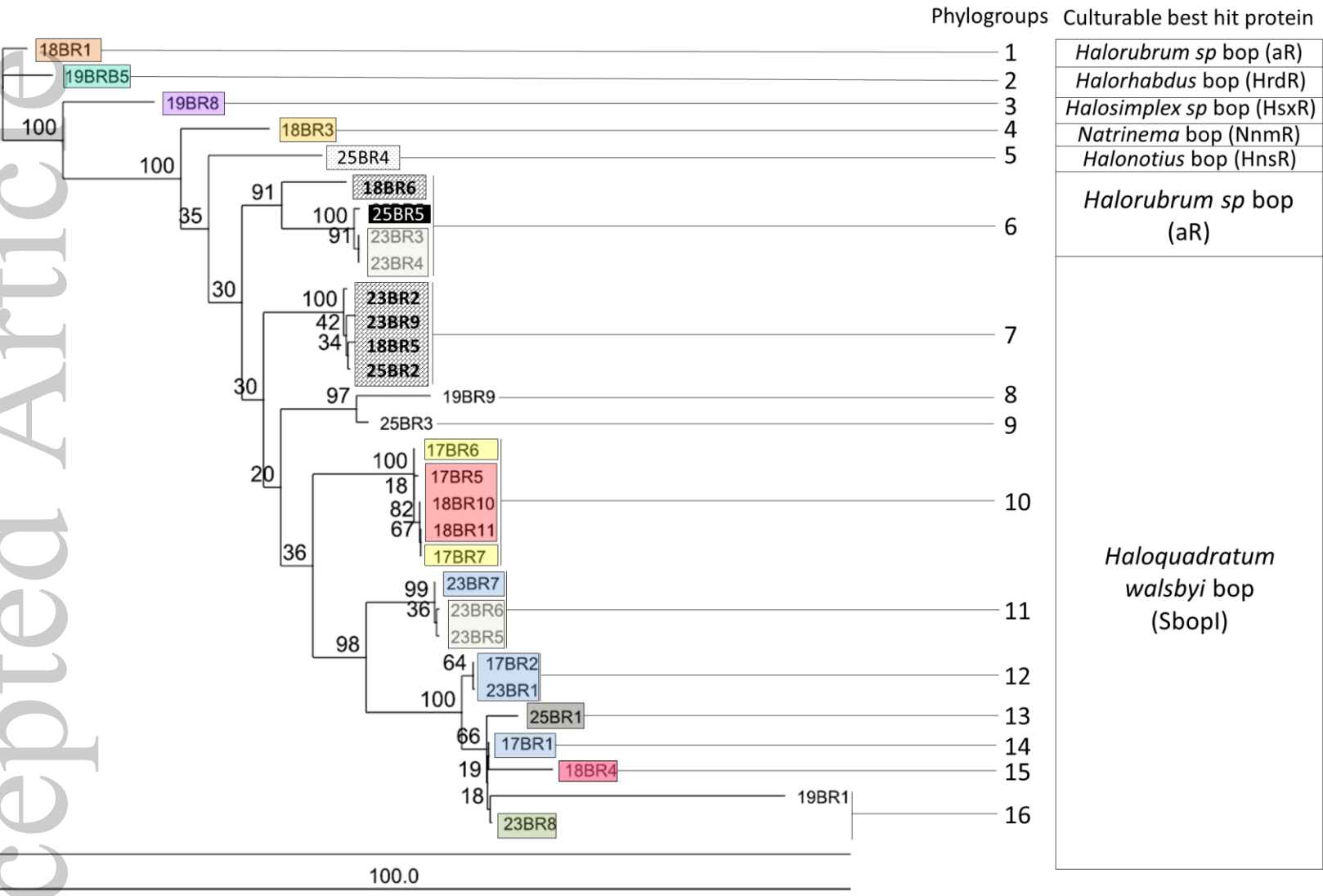
Table 1 (cont.): Retinal binding coding protein sequences retrieved in this study. Closest cultured and uncultured relative similarities are indicated as well the pond and month where/when presence of the sequences were detected in (Pond and month detected). Ponds: Medium concentrators, CMs (CM1, CM2), brine concentrator, CCAB and crystallizers, CRs (CR30 and CR41).

BACTERIORHODOPSIN-LIKE PROTEIN							
Phylogroup	Photocycle tuning protein	Sequences	Closest cultured relative (Genbank Access Number) Closest uncultured relative (Genbank Access Number)	Authors	Similarity (%)	Detected in	
						Pond	Month
10	I	17BR6,7	bacteriorhodopsin, partial [uncultured haloarchaeon](AHF27622.1)	Podell et al., 2013	91-100%	CMs	All
	IV	17BR5, 18BR10,11	bacteriorhodopsin precursor (Squarebop I) [<i>Haloquadratum walsbyi</i> DSM 16790](YP_656801.1)	Pfeiffer et al., 2008	81-83%		
11	0	23BR5, 6	bacteriorhodopsin, partial [uncultured haloarchaeon] (AGZ13722.1)	Dillon et al., 2013	97-99%	CRs	All
	VII	23BR 7	bacteriorhodopsin precursor (Squarebop I) [<i>Haloquadratum walsbyi</i> DSM 16790](YP_656801.1)	Pfeiffer et al., 2008	68-71%		
12	VII	17BR2 23BR1	bacteriorhodopsin, partial [uncultured haloarchaeon] (AHF27592.1)	Dillon et al., 2013	99%	CMs and CR30	All
			bacteriorhodopsin precursor (Squarebop I) [<i>Haloquadratum walsbyi</i> DSM 16790](YP_656801.1)	Pfeiffer et al., 2008	92%		
13	X	25BR1	bacteriorhodopsin, partial [uncultured haloarchaeon] (AHF27701.1)	Dillon et al., 2013	78%	CR41	All
			bacteriorhodopsin precursor (Squarebop I) [<i>Haloquadratum walsbyi</i> DSM 16790] (YP_656801.1)	Pfeiffer et al., 2008	79%		
14	VII	17BR1	bacteriorhodopsin, partial [uncultured haloarchaeon] (AGZ13698.1)	Papke et al., 2003	99%	CMs	MR-OC
			bacteriorhodopsin precursor (Squarebop I) [<i>Haloquadratum walsbyi</i> DSM 16790](YP_656801.1)	Pfeiffer et al., 2008	97%		
15	V	18BR4	bacteriorhodopsin, partial [uncultured haloarchaeon] AHF27701.1	Dillon et al., 2013	76%	CMs	All
			bacteriorhodopsin precursor (Squarebop I) [<i>Haloquadratum walsbyi</i> DSM 16790](YP_656801.1)	Pfeiffer et al., 2008	75%		
16		19BR1	bacteriorhodopsin, partial [uncultured Halobacteriales archaeon]AAR12458.1	Papke et al., 2003	85%	CCAB	All
			bacteriorhodopsin precursor (Squarebop I) [<i>Haloquadratum walsbyi</i> DSM 16790](YP_656801.1)	Pfeiffer et al., 2008	85%		
	IX	23BR8	bacteriorhodopsin, partial [uncultured Halobacteriales archaeon]AAR12458.1	Dillon et al., 2013	99%	CR30	All
			bacteriorhodopsin precursor (Squarebop I) [<i>Haloquadratum walsbyi</i> DSM 16790](YP_656801.1)	Pfeiffer et al., 2008	99%		

Table 1 (cont.): Retinal binding coding protein sequences retrieved in this study. Closest cultured and uncultured relative similarities are indicated as well the pond and month where/when the sequences were detected in (Pond and month detected). Ponds: Medium concentrators, CMs (CM1, CM2), brine concentrator, CCAB and crystallizers, CRs (CR30 and CR41).

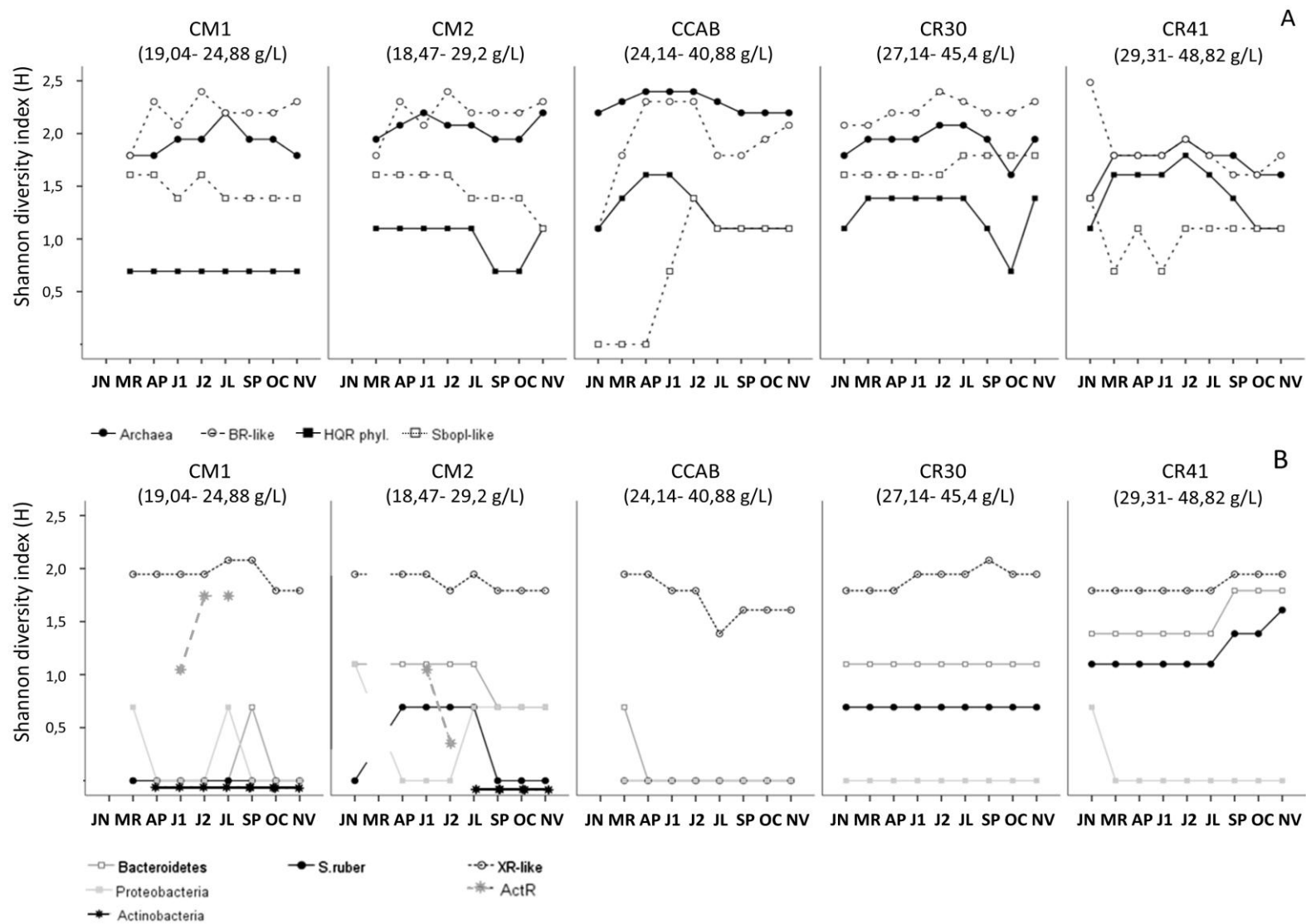
XANTHORHODOPSIN-LIKE PROTEIN (XR)						
<i>Phylogroup</i>	<i>Sequences</i>	Closest cultured relative (Genbank Access Number) Closest uncultured relative (Genbank Access Number)	<i>Authors</i>	<i>Similarity (%)</i>	<i>Presence</i>	
					<i>Pond</i>	<i>Month</i>
17	17XR2, 6, 8, 9, 10, 11 18XR2, 3, 6	Xanthorhodopsin [<i>Salinibacter ruber</i> DSM 13855] (YP_445623.1)	Mongodin et al., 2005	91-100%	All ponds	All samples
ACTINORHODOPSIN-LIKE PROTEIN (ActR)						
18	ActR1, 2, 3, 4	Putative actinorhodopsin, partial [<i>Candidatus Aquiluna rubra</i>] (ACN42845.1)	Sharma et al., 2009	77-84%	CM1 CM2	J1-JL J1-J2
		Actinorhodopsin, partial [uncultured bacterium] (CCQ25966.1)	Salka et al., 2014	77-81%		

	96	115	137	182	185	186	189	194	200	204	210	212	215	Sequences
0	D	D	W	W	Y	P	W	E	G	Y	I	D	A	23BR3, 4, 5 and 6
I	H	D	W	W	Y	P	W	E	G	Y	I	D	A	17BR6 and 7
II	D	D	W	W	Y	P	W	E	D	Y	I	D	A	18BR3
III	D	D	W	W	Y	P	W	E	S	Y	M	D	A	18BR1
IV	D	D	W	W	Y	P	W	E	S	Y	V	D	A	17BR5, 18BR10 and 11
V	D	D	W	R	Y	P	W	E	G	Y	I	D	A	18BR4
VI	D	D	W	W	Y	P	W	E	S	Y	Y	D	A	19BR8
VII	D	D	W	W	Y	P	W	E	G	Y	V	D	A	17BR2, 23BR1 and 7
VIII	D	D	W	W	Y	P	W	E	G	K	Y	D	A	19BR5
IX	D	D	W	W	Y	P	W	E	G	Y	V	D	A	23BR8
X	D	D	W	W	Y	P	W	N	G	K	G	S	A	25BR1
XI	D	D	W	W	Y	P	W	E	G	Y	G	R	R	25BR5
XII	G	D	W	W	Y	P	W	E	G	Y	I	D	A	25BR4
XIII	D	D	W	W	Y	P	W	E	N	Y	I	G	A	18BR5, 6; 23BR2, 9 and 25BR2

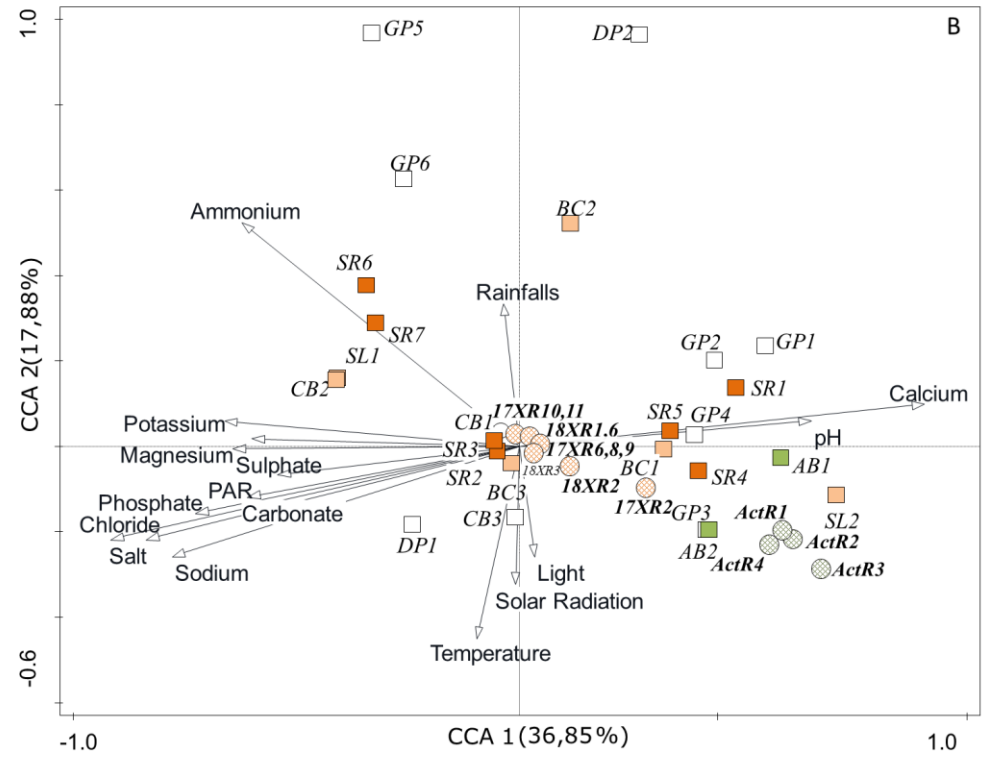
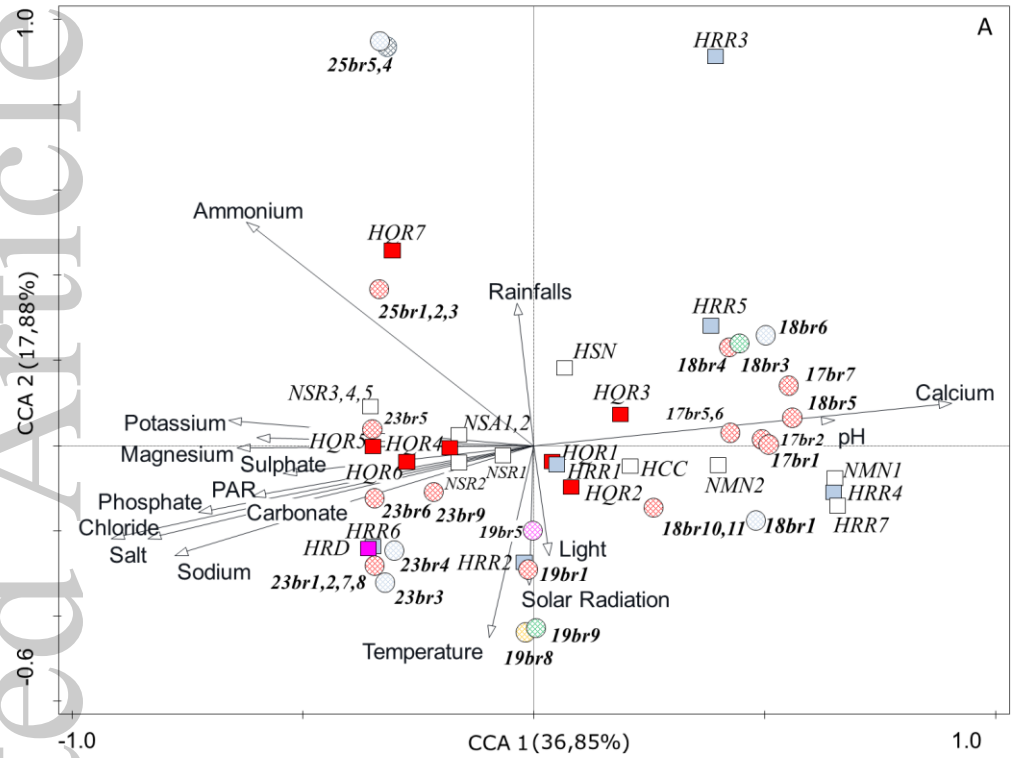


Photocycle tuning varieties	
0	Conserved PBP aminoacids
I	PBP aminoacids changed
II	
III	
IV	
V	
VI	
VII	
VIII	
IX	
X	
XI	
XII	
XIII	

EMI_12709_F1



EMI_12709_F2



Archaeal phylotypes BR producers (Gomariz et al., 2014)

- *Haloquadratum* phylotypes (HQR)
- *Halorubrum* phylotypes (aR)
- *Halorhabdus* phylotypes (HDR)
- Other archaeal phylotypes

BR-like proteins

- *Haloquadratum* bop (*SbopI*)
- *Archaerhodopsin* (aR)
- *Halorhabdus* bop (*HldR*)
- *Natrinema* bop (*NnmR*)
- *Halosimplex* bop (*HsxR*)
- *Halonotius* (*HnsR*)

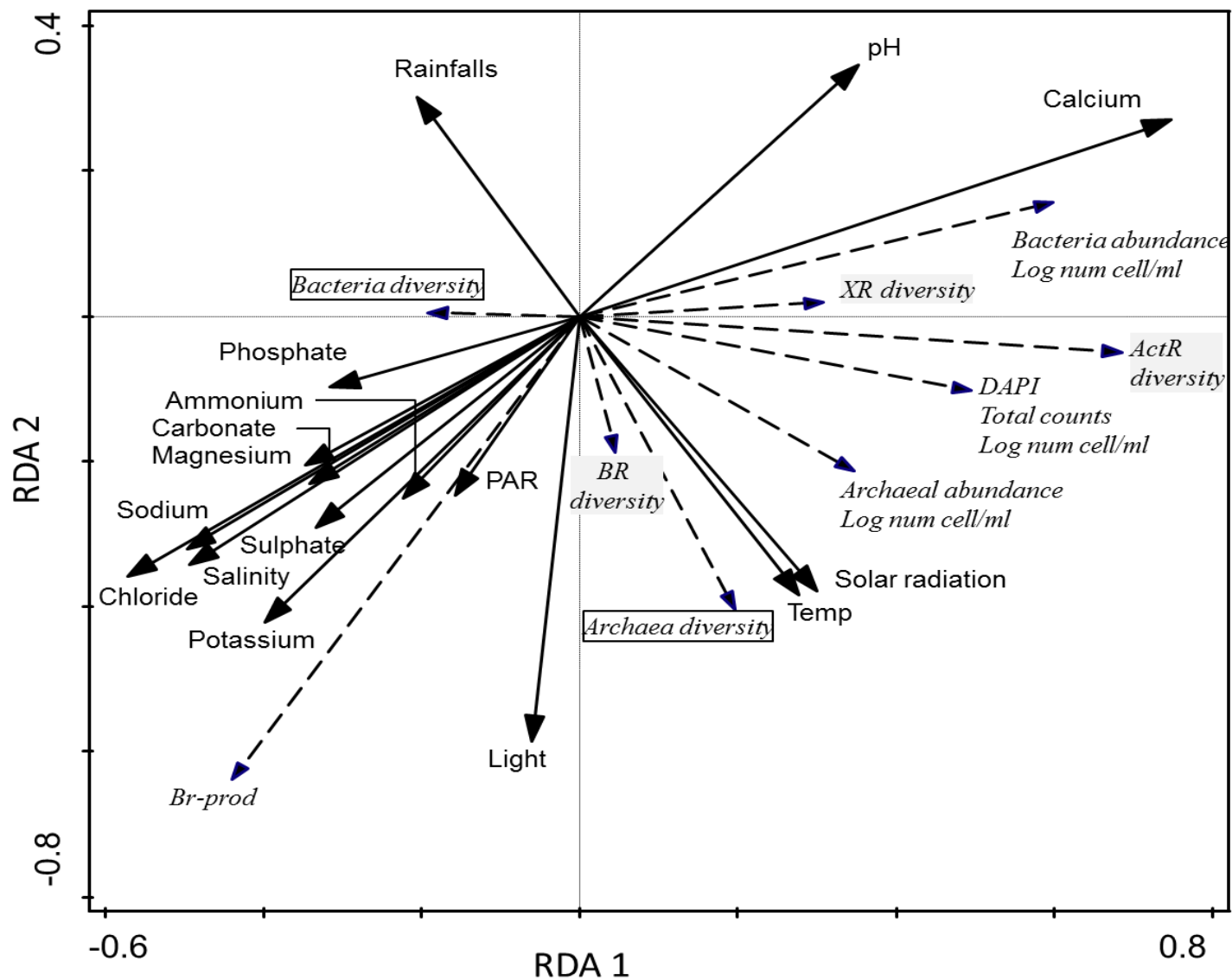
Bacterial phylotypes XR producers (Gomariz et al., 2014)

- *Salinibacter ruber* phylotypes
- *Bacteroidetes* phylotypes
- *Actinobacterial* phylotypes
- Other bacterial phylotypes

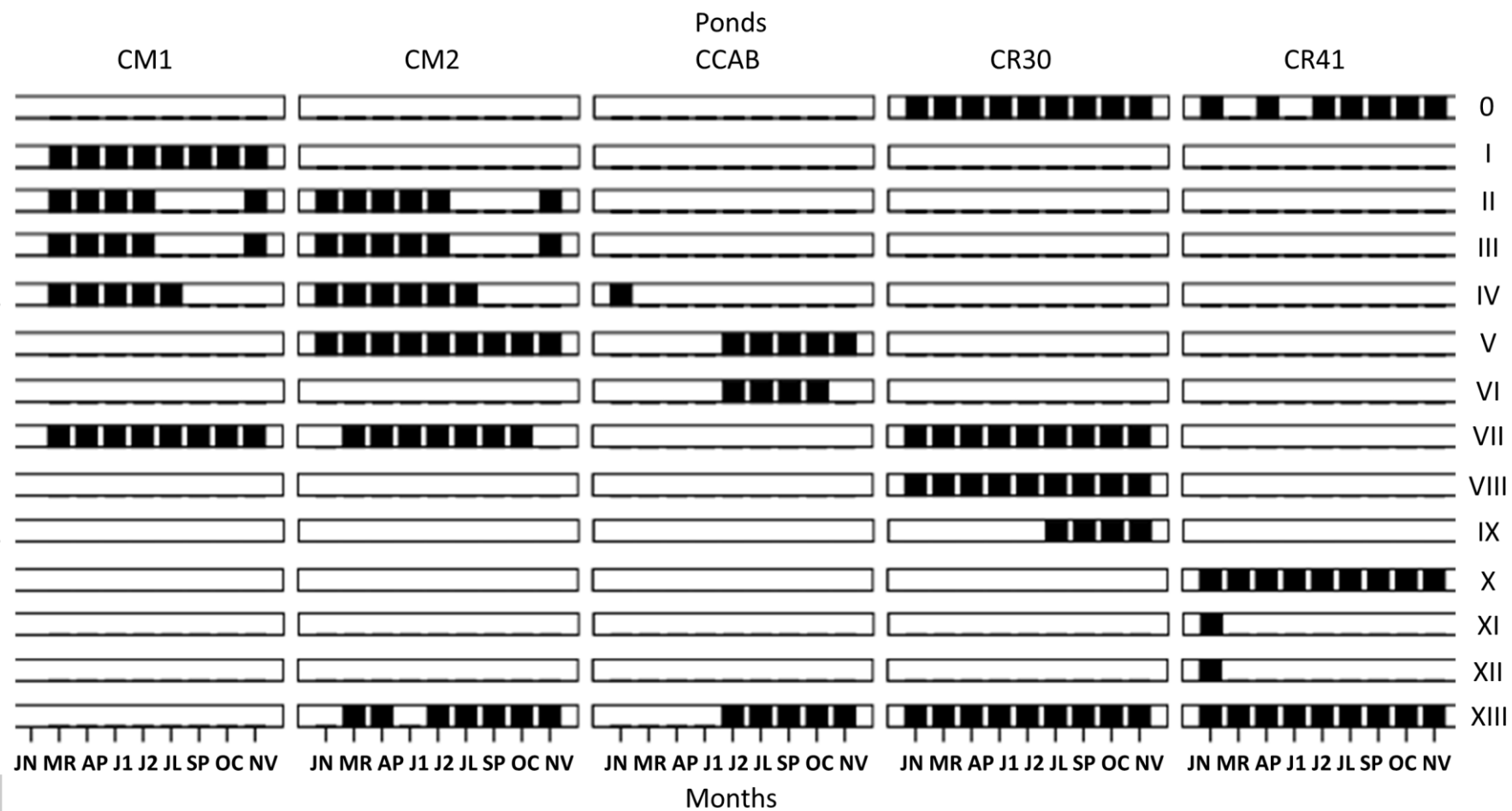
XR-like and ActR proteins

- *Xanthorhodopsin*-like proteins
- *Actinorhodopsin*-like proteins

EMI_12709_F3



EMI_12709_F4



Photocycle-tuning protein groups

EMI_12709_F5